Kidney and Blood Pressure Research

Research Article

Kidney Blood Press Res 2024;49:69–80
DOI: 10.1159/000535809

Received: January 26, 2023
Accepted: December 11, 2023
Published online: January 5, 2024

Kidney Injury by Unilateral Ureteral Obstruction in Mice Lacks Sex Differences

Samaneh Goorani[a, b] Md Abdul Hye Khan[a, c] Abhishek Mishra[b]
Ashraf El-Meanawy[d] John D. Imig[a, b]

[a]Drug Discovery Center, Medical College of Wisconsin, Milwaukee, WI, USA; [b]Department of Pharmaceutical Sciences, University of Arkansas for Medical Sciences, Little Rock, AR, USA; [c]Departments of Medical Physiology & Pharmacology, Anesthesiology, School of Medicine, University of Missouri, Columbia, MO, USA; [d]Department of Medicine, Medical College of Wisconsin, Milwaukee, WI, USA

Keywords
Renal fibrosis · Unilateral ureteral obstruction · Sex differences · Low nephron number · ROP *Os*/+ mouse

Abstract
Introduction: Renal fibrosis is a critical event in the development and progression of chronic kidney disease (CKD), and it is considered the final common pathway for all types of CKD. The prevalence of CKD is higher in females; however, males have a greater prevalence of end-stage renal disease. In addition, low birth weight and low nephron number are associated with increased risk for CKD. This study examined the development and severity of unilateral ureter obstruction (UUO)-induced renal fibrosis in male and female wild-type (ROP +/+) and mutant (ROP *Os*/+) mice, a mouse model of low nephron number. ***Methods:*** Male and female ROP +/+ and ROP *Os*/+ mice were subjected to UUO, and kidney tissue was collected at the end of the 10-day experimental period. Kidney histological analysis and mRNA expression determined renal fibrosis, tubular injury, collagen deposition, extracellular matrix proteins, and immune cell infiltration. ***Results:*** Male and female UUO mice demonstrated marked renal injury, kidney fibrosis, and renal extracellular matrix production. Renal fibrosis and α-smooth muscle actin were increased to a similar degree in ROP +/+ and ROP *Os*/+ mice with UUO of either sex. There were also no sex differences in renal tubular cast formation or renal infiltration of macrophage in ROP +/+ and ROP *Os*/+ UUO mice. Interestingly, renal fibrosis and α-smooth muscle actin were 1.5–3-fold greater in UUO-ROP +/+ compared to UUO-ROP *Os*/+ mice. Renal inflammation phenotypes following UUO were also 30–45% greater in ROP +/+ compared to ROP *Os*/+ mice. Likewise, expression of extracellular matrix and renal fibrotic genes was greater in UUO-ROP +/+ mice compared to UUO-ROP *Os*/+ mice. In contrast to these findings, ROP *Os*/+ mice with UUO demonstrated glomerular hypertrophy with 50% greater glomerular tuft area compared to ROP +/+ with UUO. Glomerular hypertrophy was not sex-dependent in any of the genotypes of ROP mice. These findings provide evidence that low nephron number contributes to UUO-induced glomerular hypertrophy in ROP *Os*/+ mice but does not enhance renal fibrosis, inflammation, and renal tubular injury. ***Conclusion:*** Taken together, we demonstrate that low nephron number contributes to enhanced glomerular hypertrophy but not

karger@karger.com
www.karger.com/kbr

Correspondence to:
John D. Imig, jimig@uams.edu

kidney fibrosis and tubular injury. We also demonstrate that none of the changes caused by UUO was affected by sex in any of the ROP mice genotypes.

Introduction

Chronic kidney disease (CKD) is one of the most prominent causes of death and suffering in the 21st century. Due to the rise in risk factors, such as obesity and diabetes, the number of patients affected by CKD has been increasing. In 2017, an estimated 844 million individuals were suffering from CKD worldwide. Like many human diseases, a prominent role of sexual dichotomy is reported in the development and progression of kidney disease including CKD [1–4]. Interestingly, the prevalence of CKD in the USA is higher in female than males; however, males progress to end-stage renal disease (ESRD) in greater numbers [5, 6]. Reduced nephron number which is associated with abnormally small kidneys with normal morphology also accounts for a significant proportion of CKD cases in children and is an inborn cause of CKD in adults [7]. Despite the seriousness, there are limited experimental animal studies on sex differences and the impact of low nephron number to the progression of CKD.

Unilateral ureter obstruction (UUO) model is used to cause progressive renal fibrosis characterized by tubular injury and interstitial inflammation which occurs in CKD [8, 9]. Renal interstitial fibrosis is the final common pathway by which CKD progresses to ESRD [10]. This process is dynamic and characterized by activation of renal interstitial fibroblasts and excessive accumulation of extracellular matrix proteins [11]. The histopathology of renal interstitial fibrosis features deposition of the extracellular matrix components, loss of tubular cells, and accumulation of fibroblasts [12]. CKD progression and renal fibrosis are also often associated with nephron loss. During nephron loss, net glomerular filtration rate is maintained by the remaining nephrons, which are compensated through glomerular hypertrophy [13, 14]. Glomerular hypertrophy is thought to precipitate in the further damage to the remaining nephrons, leading to renal failure [14]. However, the impact of biological sex and lifelong low nephron number on UUO kidney fibrosis has not yet been extensively evaluated.

In this study, we evaluated UUO-induced renal fibrosis in male and female ROP +/+ and mutant ROP Os/+ mice, a mouse model of low nephron numbers. The heterozygote Os/+ mice (ROP *Os*/+) have a skeletal phenotype mainly in the form of fused digits (oligosyndactyly) and a renal phenotype in the form of 50% reduction in nephron number, whereas their +/+ littermates (ROP +/+) have normal phenotypes [15–17]. Although the UUO model has been extensively utilized for CKD, there have been limited studies on sex differences. UUO experimental studies in rodents have found either increased kidney injury in males or no sex differences [18–21]. The main aim of this study was to test the hypothesis that there would be an enhanced UUO-induced renal fibrosis, tubular injury, and inflammation in male mice. This study also tested the hypothesis that UUO-induced kidney fibrosis and injury will be higher in low nephron number ROP *Os*/+ mice than normal ROP +/+ mice. Surprisingly, we found that except for a marked effect on glomerular size, UUO-induced renal effects were similar in male and female mice of both genotypes, and low nephron number does not enhance renal tubular injury following UUO.

Materials and Methods

All chemicals used in this study were purchased from Sigma-Aldrich (St. Louis, MO, USA) unless mentioned otherwise.

Animal Experiments

All experiments of this study were approved (protocol # AUA 2031) and carried out according to guidelines of the Institutional Animal Care and Use Committee of the Medical College of Wisconsin. In the present study, we utilized a mouse model of low renal mass, the ROP *Os*/+ mice. The ROP/Le-*Os* Ces1ca/+ Ces1ca/J oligosyndactyly (ROP *Os*/+) (Strain #002503) was established at the Jackson Laboratory and has been maintained by sibling mating. We obtained this strain via Cryo Recovery from the Jackson Laboratory (Bar Harbor, ME) and mated with wild-type C57Bl/6J at the Jackson Laboratory (Bar Harbor, ME) for at least 10 generations. The mutant ROP *Os*/+ and its wild-type littermate ROP +/+ mice were bred at the Medical College of Wisconsin. Male and female mice between 17 and 23 weeks of age were used for these studies. UUO surgery was done in anesthetized mice under sterile surgical conditions. Mice were anesthetized with 2.0% isoflurane, and UUO was carried out with the left ureter obstructed completely one-third distal from the renal pelvis using a 6–0 silk tie [22, 23]. Sham-surgery mice went through the same surgical procedure as the UUO mice except for the ureter ligation. Analgesia, buprenorphine sustained release (1 mg/kg, ZooPharm, Fort Collins, CO), was given prior to recovery from anesthesia. Mice of either sex were divided into four groups (n = 12–20/group/sex) as control ROP +/+, UUO-ROP +/+, control ROP *Os*/+, and UUO-ROP *Os*/+. At the end of the 10-day experimental protocol, kidney tissue was collected under isoflurane anesthesia for histopathological and other analysis, and the mice were euthanized.

Histopathology

Kidney tissues were fixed in 10% buffered formalin, sectioned (5 μm) and were stained with Picrosirius red (PSR), hematoxylin and eosin (HE) or Periodic Acid-Schiff (PAS) (Alfa Aesar, Tewksbury, MA, USA) for histological examination using ×200 magnification and NIS Elements AR version 3.0 (Nikon Instruments Inc., Melville, NY, USA) imaging software. Kidney fibrosis was determined in PSR-stained sections and data presented as kidney area positive for collagen. The percentage area positive for interstitial collagen was calculated from the mean of 20 cortical and 10 medullary fields for each animal. The percentage area positive for proteinaceous cast was calculated from the mean of eight cortical and five medullary fields for each animal. Glomerular tuft area was calculated from PAS-stained slides. Twenty glomeruli were measured from each kidney sample by two blinded observers, and the average glomerular tuft area was determined. Glomeruli per kidney cortical area were determined in each experimental group. The number of glomeruli is expressed as the average number of glomeruli calculated from ten 10 mm^2 fields from the kidney sample of each mouse using Aperio eSlide Manager (Leica Biosystems, Deer Park, IL, USA) in a blinded fashion by two observers.

Immunohistopathological Analysis

For immunohistological analysis, formalin-fixed paraffin-embedded kidney tissues were deparaffinized, rehydrated, and stained with anti-α-smooth muscle actin (α-SMA) (1:100, Santa Cruz Biotechnology, Dallas, TX, USA) or anti-MAC2 (1:100, Santa Cruz Biotechnology) antibodies overnight and at 4°C. On the second day, the kidney sections were washed and incubated with biotinylated anti-mouse secondary antibody (1:200) for 1 h. Finally, α-SMA and MAC2-positive signals were developed using avidin-biotinylated HRP complex (VECTASTAIN ABC Elite kit, Vector Laboratories, Burlingame, CA, USA) followed by counterstaining with hematoxylin. Kidney tissue slides were mounted, and the immunostained kidney sections were examined at ×400 magnification with a light microscope and analyzed using Nikon NIS Elements Software (Nikon Instruments Inc., Melville, NY, USA). The MAC2- and α-SMA-positive renal section areas were examined by two blinded observers and expressed as the percentage area fraction relative to the total area analyzed.

Real-Time PCR Analysis

Kidney mRNA expression of fibrotic markers α-SMA (*Acta2*) and fibronectin (*Fn1*), a fibrosis regulatory marker zinc finger E-box binding homeobox 1 Zeb-1 (*Zeb1*), and renal tubular injury marker neutrophil gelatinase-associated lipocalin (NGAL) (*LCN2*) were carried out using Real-Time PCR (RT-PCR) analysis. Isolation of total RNA and preparation of mRNA were carried out using RNeasy Mini Kit (QIAGEN, CA, USA) according to the manufacturer's instructions to prepare the messenger RNA (mRNA) from each sample homogenate. The mRNA samples were quantified spectrophotometrically at 260 nm. The iScript™ Select cDNA Synthesis Kit (Bio-Rad, Hercules, CA, USA) was used to reverse-transcribed 1 μg of RNA to cDNA. Target gene expression was quantified by iScript One-Step RT-PCR Kit with SYBR green using the MyiQ™ Single Color Real-Time PCR Detection System (Bio-Rad Laboratories, Hercules, CA, USA). Using a dissociation curve analysis with the iQ5 Optical System Software, Version 2.1 (Bio-Rad Laboratories, Hercules, CA, USA), each amplified sample was analyzed for homogeneity. After denaturation at 95°C for 2 min, 40 cycles were performed at 95°C for 10 s and at 60°C for 30 s. Each sample was run in triplicate and to examine the relative expression of the target genes, and the C_t values were normalized compared to two housekeeping genes, *Pgk1* and *Actb*. Comparative threshold cycle (C_t) method between experimental and control mice groups was used to quantify a fold increase ($2^{-\Delta\Delta Ct}$) in the expression of the target genes.

Statistical Analysis

Statistical significance between groups was determined using 3-way ANOVA using GraphPad Prism® Version 9.0 software (GraphPad Software Inc., La Jolla, CA, USA). Data are reported in scattered plot (all individual data) format with mean and standard error of mean (SEM). The significance of 3-way ANOVA was considered significant ($p < 0.05$) for sex, genotypes, and UUO surgery. The $p < 0.05$ was also considered significant for the difference between experimental groups.

Results

Renal Fibrosis in ROP +/+ and ROP Os/+ Male and Female Mice following UUO

UUO-induced renal fibrosis in male and female ROP +/+ and ROP *Os*/+ mice. PSR staining in the kidney sections demonstrated UUO-induced renal cortical collagen deposition in male and female mice of both genotypes. Following UUO, the ROP +/+ mice had greater cortical collagen-positive area and averaged at 17.5% compared to 9% in ROP *Os*/+ mice (Fig. 1a), and cortical collagen formation was similar between male and female mice of both genotypes (Fig. 1a–c). Like in the cortex, UUO-induced medullary collagen-positive area was greater in ROP +/+ (1.6-fold higher than sham mice) compared to that in ROP *Os*/+ mice (3–3.5-fold higher than sham) (Fig. 2a). Interestingly, sex did not affect the UUO-induced renal medullary collagen formation in both mouse genotypes (Fig. 2a–c).

Kidney immunohistochemical analysis of the myofibroblast marker α-SMA was carried out in male and female ROP +/+ and ROP *Os*/+ mice following UUO. Renal cortical deposition of the fibrotic and myofibroblast marker α-SMA was higher in male and female UUO-ROP +/+ and UUO-ROP *Os*/+ mice compared respective sham mice (Fig. 3a–c). Like collagen deposition, the renal α-SMA deposition was approximately 2-fold higher in ROP +/+ compared with ROP *Os*/+ mice, and sex did not affect renal α-SMA deposition in both genotypes following UUO (Fig. 3a–c).

Renal expression of a set of prominent fibrotic genes was also studied in ROP +/+ and ROP *Os*/+ mice with or without UUO. Kidney mRNA expression of α-SMA (*Acta2*), fibronectin (*Fn1*), and ZEB-1 (*Zeb1*) was higher

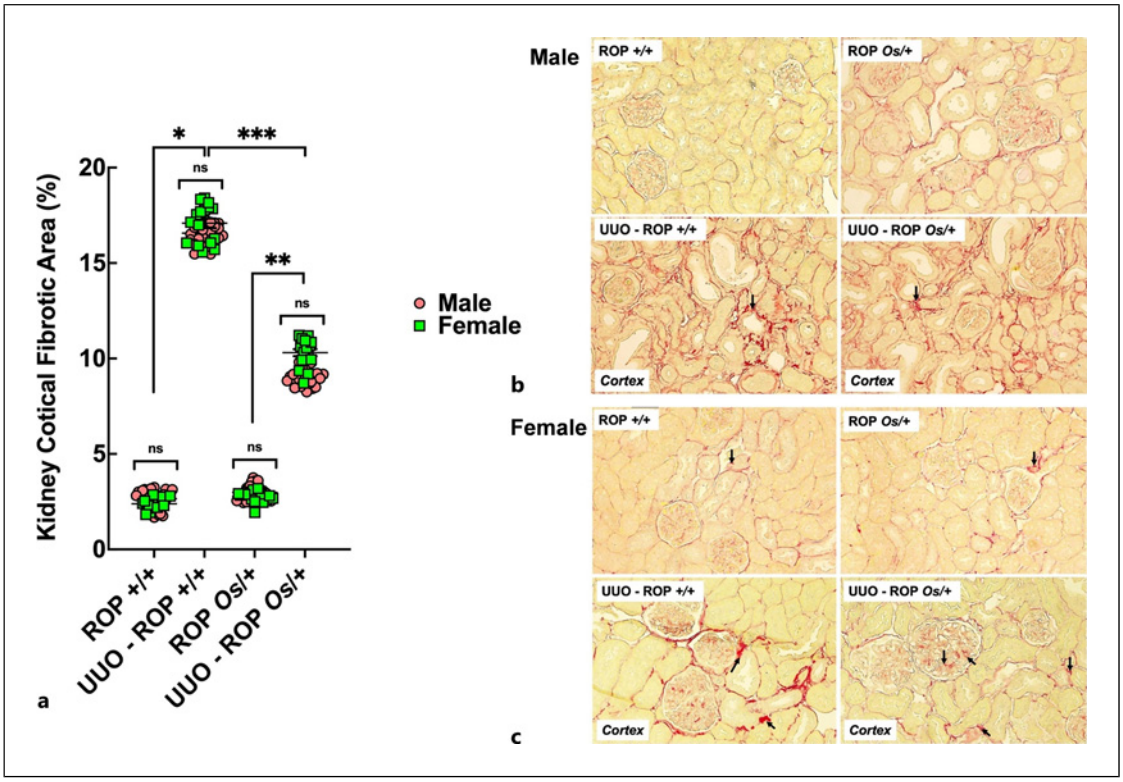

Fig. 1. Unilateral ureter obstruction (UUO) caused cortical fibrosis in ROP +/+ and ROP *Os*/+ mice. **a** Renal collagen deposition in the kidney cortex of male and female mice of both genotypes. Representative photomicrograph depicting collagen-positive area identified using PSR stain in male (**b**) and female (**c**) mice. Scale bar = 100 μm. Black arrows indicated collagen-positive fibrotic area. Data were analyzed by 3-way ANOVA and presented in scattered plot format with mean and SEM. Data were analyzed by 3-way ANOVA and presented in scattered plot format with mean and SEM. The 3-way ANOVA was significant ($p < 0.05$) for UUO and genotype (ROP+/+ vs. ROP Os/+) but not ($p > 0.05$) for the sex of the mice. *$p < 0.05$ ROP +/+ versus UUO-ROP +/+; **$p < 0.05$ ROP *Os*/+ versus UUO-ROP *Os*/+; ***$p < 0.05$ UUO-ROP +/+ versus UUO-ROP *Os*/+; n = 20/group from two sets of experiments; ns = not significant.

in both sexes of ROP +/+ compared to ROP *Os*/+ mice. UUO caused 3–3.5-fold higher renal α-SMA expression in ROP +/+ compared to ROP *Os*/+ mice irrespective of sex (Fig. 4a). Like α-SMA, renal expression of *Zeb1* (Fig. 4b) was 3–4-fold and *Fn1* (Fig. 4c) expression was 2-fold higher in male and female ROP +/+ compared to ROP *Os*/+ mice. Overall, these data demonstrate a lack of sex differences in renal fibrosis, α-SMA levels, and expression of fibrotic genes following UUO. We also demonstrate that low nephron number did not exacerbate UUO-induced renal fibrosis and tubular injury in mice.

UUO Renal Tubular Injury in ROP +/+ and ROP Os/+ *Mice*

Marked renal tubular injuries including tubular necrosis, swelling of the renal tubules, and tubular cast formation were evident in male and female ROP +/+ and ROP *Os*/+ mice following UUO. UUO-induced renal tubular cast formation was greater in ROP +/+ compared with ROP *Os*/+ mice. The tubular injury in these mice was not dependent on sex as the extent of injury was similar between male and female mice (Fig. 5b–d). Like renal tubular cast formation, following UUO, gene expression of tubular injury markers NGAL was higher in ROP +/+ compared with ROP *Os*/+ mice and was not sex dependent (Fig. 5a). Overall, these findings demonstrate that, irrespective of sex, the ROP +/+ mice developed greater UUO-induced renal tubular injury and cast formation compared to ROP *Os*/+ mice.

Kidney Inflammation in ROP +/+ and ROP Os/+ *Mice following UUO*

Renal infiltration of immune cells including macrophages is an important pathophysiological event in fibrosis and renal tubular injury [24]. Kidney

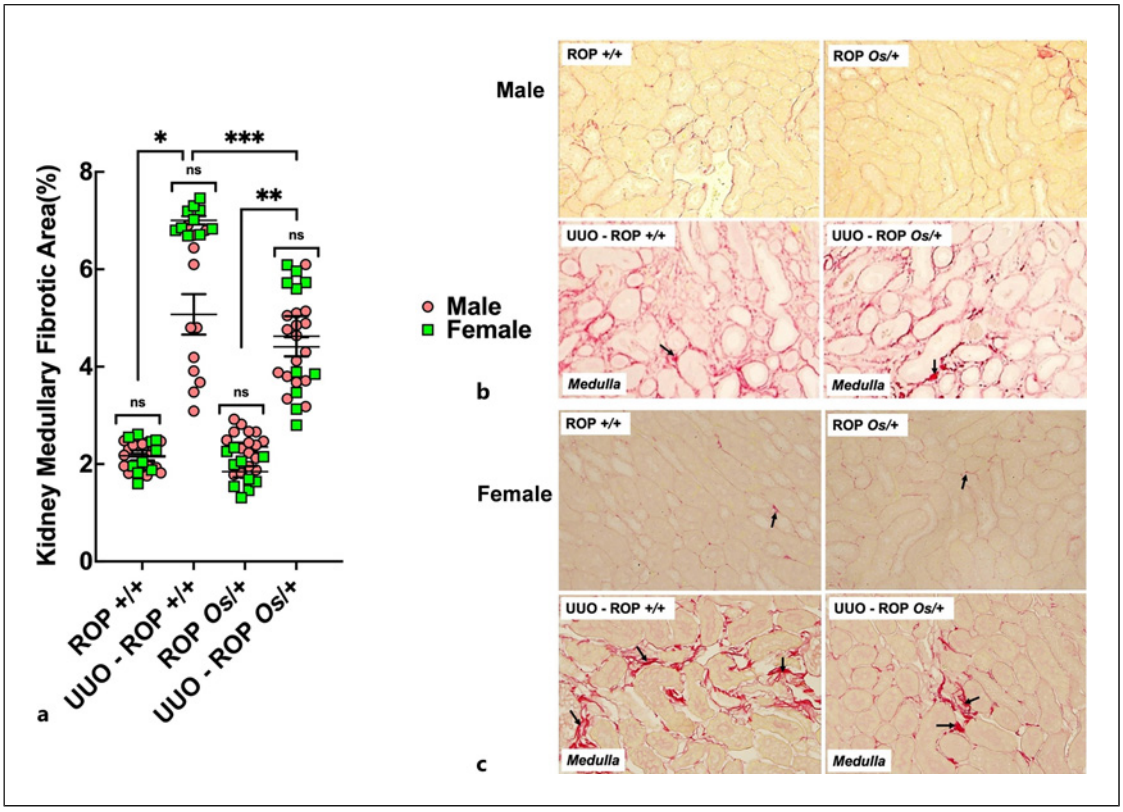

Fig. 2. Unilateral ureter obstruction (UUO) caused medullary fibrosis in ROP +/+ and ROP *Os*/+ mice. **a** Renal collagen deposition in kidney medulla of male and female mice of both genotypes. Representative photomicrograph depicting collagen-positive area identified using PSR stain in male (**b**) and female (**c**) mice. Scale bar = 100 μm. Black arrows indicated collagen-positive fibrotic area. Data were analyzed by 3-way ANOVA and presented in scattered plot format with mean and SEM. The 3-way ANOVA was significant ($p < 0.05$) for UUO and genotype (ROP+/+ vs. ROP Os/+) but not ($p > 0.05$) for the sex of the mice. *$p < 0.05$ ROP +/+ versus UUO-ROP +/+; **$p < 0.05$ ROP *Os*/+ versus UUO-ROP *Os*/+; ***$p < 0.05$ UUO-ROP +/+ versus UUO-ROP *Os*/+; $n = 18$/group from two sets of experiments; ns, not significant.

immunohistochemical analysis of MAC2 was carried out in male and female ROP +/+ and ROP *Os*/+ mice following UUO. Renal MAC2 levels were elevated in UUO-ROP +/+ and UUO-ROP *Os*/+ mice compared to their respective sham control groups (Fig. 6a–c). Consistent with renal fibrosis and tubular injury, MAC2-positive macrophages in male and female UUO-ROP +/+ mice were greater when compared to male and female UUO-ROP *Os*/+ mice. Likewise, the sex of the mice did not affect the UUO-induced increase in renal MAC2 levels as macrophage accumulation was similar in male and female ROP +/+ and ROP *Os*/+ mice (Fig. 6a–c). These findings demonstrate that UUO-induced renal inflammation to a similar extent in male and female mice and that UUO increased renal inflammation to a greater extent in ROP +/+ mice compared to low nephron number ROP *Os*/+ mice.

Glomerular Tuft Area in ROP +/+ and ROP Os/+ *Mice following UUO*

Glomerular tuft area was measured in male and female ROP +/+ and ROP *Os*/+ mice following UUO. The glomerular tuft area was higher in ROP *Os*/+ compared to ROP +/+ mice with UUO. Our data also demonstrated that UUO-induced change in glomerular tuft area for either genotype of ROP mice was not affected by the gender of the mice (Fig. 7).

Discussion

CKD is major healthcare issue that affects females in greater numbers; however, progression of CKD to ESRD is greater in males [5, 6]. There have been a limited number of experimental studies determining sex differences in kidneys of UUO rodents because male rodents are preferred over female rodents where the reproductive

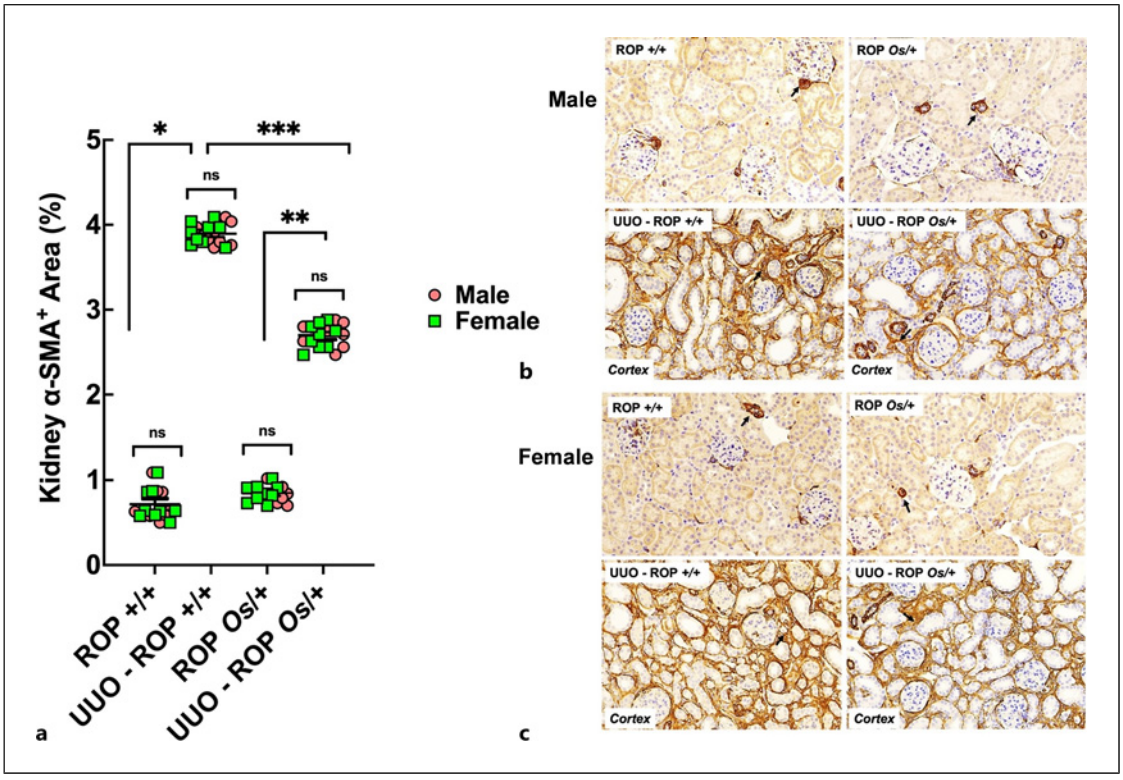

Fig. 3. Unilateral ureter obstruction (UUO) elevated α-smooth muscle actin (α-SMA) in ROP +/+ and ROP *Os*/+ mice. **a** Renal collagen deposition in the kidney medulla of male and female mice of both genotypes. Representative photomicrograph depicting α-SMA-positive area identified using immunohistology in male (**b**) and female (**c**) mice. Scale bar = 100 μm. Data were analyzed by 3-way ANOVA and presented in scattered plot format with mean and SEM. Data were analyzed by 3-way ANOVA and presented in scattered plot format with mean and SEM. The 3-way ANOVA was significant ($p < 0.05$) for UUO and genotype (ROP+/+ vs. ROP Os/+) but not ($p > 0.05$) for the sex of the mice. *$p < 0.05$ ROP +/+ versus UUO-ROP +/+; **$p < 0.05$ ROP *Os*/+ versus UUO-ROP *Os*/+; ***$p < 0.05$ UUO-ROP +/+ versus UUO-ROP *Os*/+; $n = 8$/group from two sets of experiments; ns, not significant.

organs complicate the UUO surgical procedure [9]. These limited studies evaluating sex differences in the UUO kidney disease model have resulted in conflicting results [18–21]. Another factor that can alter CKD progression is low nephron number, and this occurs with low birth weight and premature birth [7]. The current study in UUO mice determined sex differences and the impact of low nephron number to the progression of CKD. UUO was induced for 10 days in males and females of two strains of mice, ROP +/+ and ROP *Os*/+ mice. ROP *Os*/+ mice harbor the oligosyndactylism (Os) radiation-induced alleles, have a mutation in chromosome 8, and disrupt the Anapc10 (Apc10/Doc1) gene [25]. This leads to developmental defects which include fusion of the second and third digits in all paws and a 50% reduction in renal nephron number [15–17]. The findings of our experimental study demonstrate limited sex differences in kidney tubular and fibrotic injury in ROP +/+ and ROP *Os*/+ mouse strains subjected to UUO. An unexpected finding was that low nephron number ROP *Os*/+ mice subjected to UUO had lesser levels of renal fibrosis and inflammation compared to ROP +/+ mice.

In the progression of renal disease, renal fibrosis is the final common pathway for most forms of progressive renal disease leading to ESRD [26, 27]. Understanding the pathophysiology of renal fibrosis is critical in the treatment and management of renal disease [28]. The UUO model causes rapid development of renal fibrosis in rodents [29–31]. In the present study, we investigated development of renal fibrosis in male and female ROP +/+ and low nephron number ROP *Os*/+ mice. Our findings demonstrated marked renal fibrosis with kidney collagen deposition after 10 days following UUO surgery in ROP +/+ and ROP *Os*/+ mice. In several earlier studies, others and we reported marked renal fibrosis with increased renal collagen deposition in response to UUO [22–24]. Renal fibrosis characterized by elevated expression of a prominent extracellular matrix protein, fibronectin, was evident

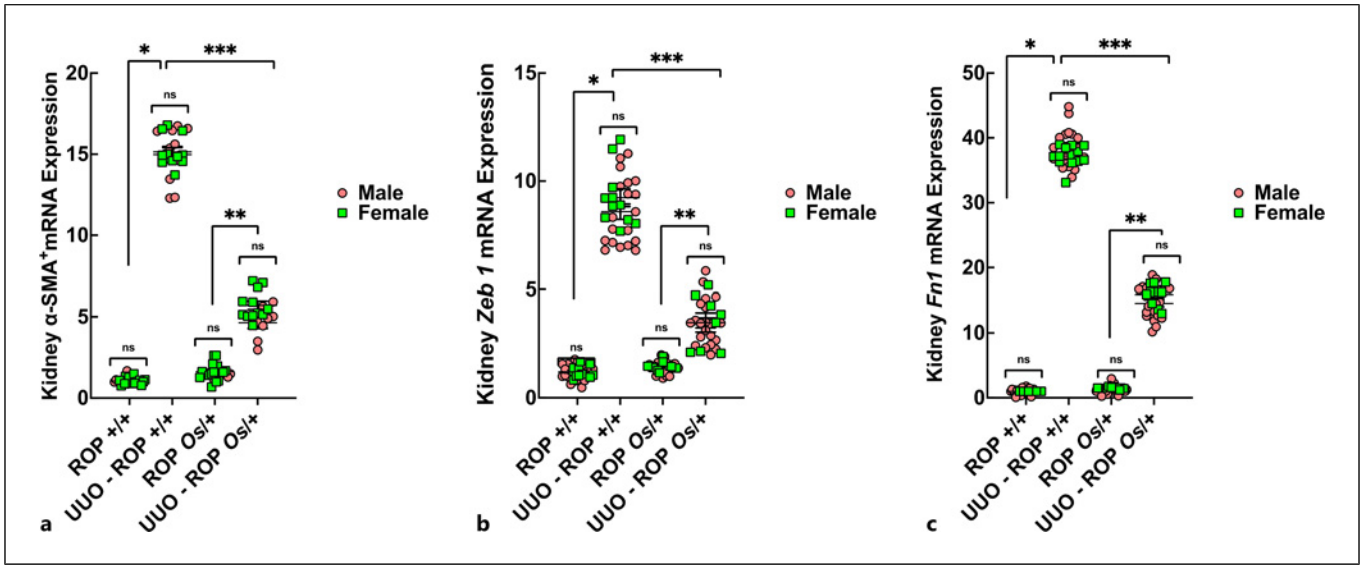

Fig. 4. Unilateral ureter obstruction (UUO) elevated renal fibrotic gene expression in ROP +/+ and ROP *Os*/+ mice. Renal mRNA expression of α-smooth muscle actin SMA (α-SMA, *Acta2*) (**a**), zinc finger E-box binding homeobox 1 Zeb-1 (*Zeb1*) (**b**), and fibronectin (*Fn1*) (**c**) in the kidney of male and female mice of both genotypes. Data were analyzed by 3-way ANOVA and presented in scattered plot format with mean and SEM. Data were analyzed by 3-way ANOVA and presented in scattered plot format with mean and SEM. The 3-way ANOVA was significant ($p < 0.05$) for UUO and genotype (ROP+/+ vs. ROP Os/+) but not ($p > 0.05$) for the sex of the mice. *$p < 0.05$ ROP +/+ versus UUO-ROP +/+; **$p < 0.05$ ROP *Os*/+ versus UUO-ROP *Os*/+; ***$p < 0.05$ UUO-ROP +/+ versus UUO-ROP *Os*/+; n = 18/group from two sets of experiments; ns, not significant.

following UUO in ROP +/+ and ROP *Os*/+ mice. Elevated level of extracellular matrix proteins responsible for fibrinogenesis has been reported in UUO and other CKD rodent models [19, 29]. The findings of the current study failed to find significant sex differences in kidney damage induced by UUO in two mouse strains. Interestingly, the findings of the current study demonstrate that ROP +/+ mice have higher renal expression of fibronectin with greater renal fibrosis and collagen deposition compared to low nephron number ROP *Os*/+ mice.

Apart from collagen deposition and extracellular matrix protein expression, the relative presence of myofibroblast in the kidney of ROP +/+ and ROP *Os*/+ mice was evaluated. It is widely reported that myofibroblasts play critical role in the pathophysiology of organ fibrosis including kidney fibrosis [32, 33]. Renal interstitial fibroblasts and myofibroblasts are largely responsible for producing excessive extracellular matrix proteins in the fibrotic kidney [32, 33]. The more severe the degree of fibrosis, the more myofibroblasts present in the kidney [32]. Myofibroblasts are long-term activated fibroblasts that express α-SMA [19, 29]. Findings in the current study demonstrate that renal fibrosis in ROP +/+ and ROP *Os*/+ mice in response to UUO was accompanied by elevated α-SMA. Like renal fibrosis, our data demonstrate that renal α-SMA expression was higher in ROP +/+ compared to low nephron number ROP *Os*/+ mice. Renal ZEB-1 expression that regulates myofibroblast formation and fibrotic process was also elevated in ROP +/+ compared to ROP *Os*/+ mice. In ROP *Os*/+ mice, the lower expression of ZEB-1 could be related to lower renal fibrosis and myofibroblast formation. Overall, these findings clearly indicate that development of renal fibrosis in response to UUO was not enhanced in mice with lower renal mass.

In the present study, it was found that UUO-induced renal fibrosis, α-SMA, and genes regulating myofibroblast formation lacked sex differences in ROP +/+ and low nephron number ROP *Os*/+ mice. This finding is contrary to the predominant human evidence that suggests that CKD progresses faster in males than females [6, 34]. Increased testosterone has been suggested as a critical factor for increased CKD progression in males. Likewise, UUO in male and testosterone-treated oophorectomized female rats demonstrated increased tubulointerstitial fibrosis and renal dysfunction compared with castrated males and normal female rats [19]. Renal inflammation and oxidative stress in male rodents could contribute to this increase in UUO-induced kidney damage [18, 19]. On the other hand, an experimental study found that UUO-induced renal fibrosis and α-SMA were similar between male and female C57Bl6/J

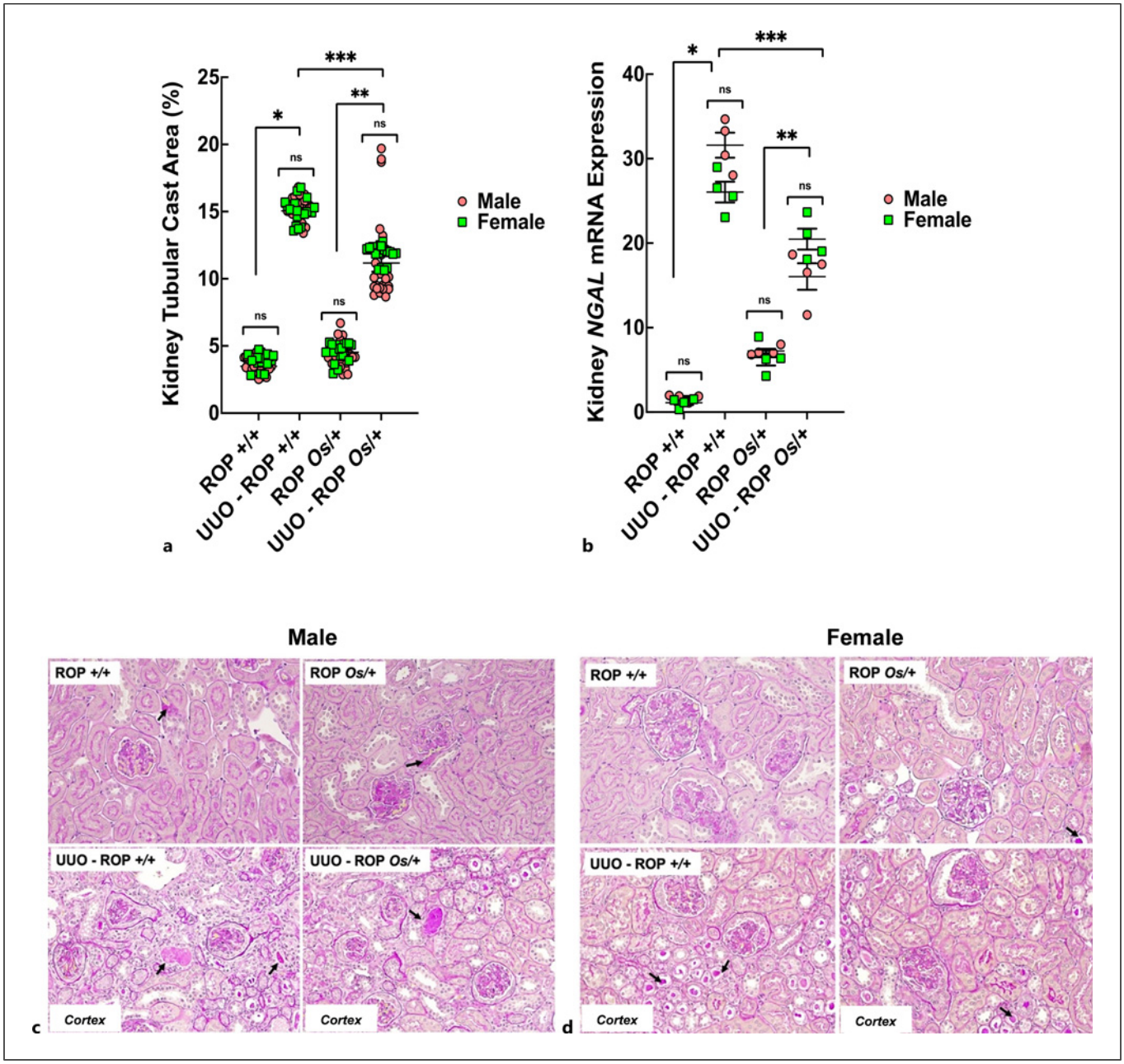

Fig. 5. Unilateral ureter obstruction (UUO) elevated tubular injury in ROP +/+ and ROP *Os*/+ mice. **a** Renal tubular cast formation in the kidney of male and female mice of both genotypes. **b** Renal mRNA expression of NGAL (*LCN2*) in the kidney of male and female mice of both genotypes. **c**, **d** Representative photomicrographs showing tubular injury and cast formation in different experimental groups of male and female mice, respectively. Scale bar = 100 μm. Black arrows indicated tubular cast area. Renal gene expression of tubular injury markers NGAL (**d**) in different experimental groups. Data were analyzed by 3-way ANOVA and presented in scattered plot format with mean and SEM. Data were analyzed by 3-way ANOVA and presented in scattered plot format with mean and SEM. The 3-way ANOVA was significant ($p < 0.05$) for UUO and genotype (ROP+/+ vs. ROP Os/+) but not ($p > 0.05$) for the sex of the mice. *$p < 0.05$ ROP +/+ versus UUO-ROP +/+; **$p < 0.05$ ROP *Os*/+ versus UUO-ROP *Os*/+; ***$p < 0.05$ UUO-ROP +/+ versus UUO-ROP *Os*/+; $n = 20$/group from two sets of experiments; ns, not significant.

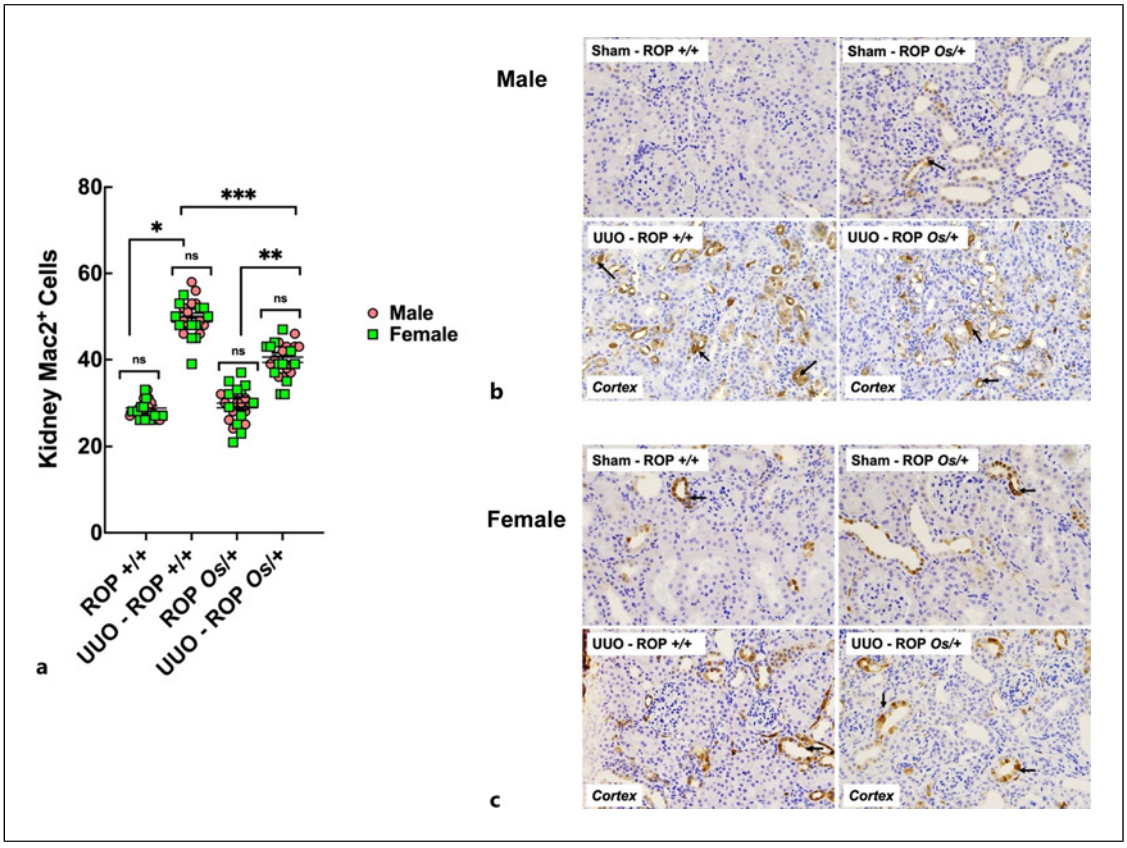

Fig. 6. Unilateral ureter obstruction (UUO) caused renal inflammation in ROP +/+ and ROP *Os*/+ mice. **a** Renal deposition of MAC2-positive macrophages in the kidney of male and female mice of both genotypes. Representative photomicrograph depicting macrophages identified using immunohistology in male (**b**) and female (**c**) mice. Scale bar = 100 μm. Black arrows indicated MAC2 positive cells. Data were analyzed by 3-way ANOVA and presented in scattered plot format with mean and SEM. Data were analyzed by 3-way ANOVA and presented in scattered plot format with mean and SEM. The 3-way ANOVA was significant ($p < 0.05$) for UUO and genotype (ROP+/+ vs. ROP Os/+) but not ($p > 0.05$) for the sex of the mice. *$p < 0.05$ ROP +/+ versus UUO-ROP +/+; **$p < 0.05$ ROP *Os*/+ versus UUO-ROP *Os*/+; ***$p < 0.05$ UUO-ROP +/+ versus UUO-ROP *Os*/+; n = 13/group from two sets of experiments; ns, not significant.

and cyclooxygenase-2 −/− mice [21, 35]. The lack of sex differences was also observed in Wistar rats following 7 days of UUO [20]. Findings of the current experimental study demonstrate at UUO day 10 that renal cortical fibrosis, α-SMA, and genes regulating myofibroblast formation were similar between male and female ROP +/+ and ROP *Os*/+ mice.

The rodent UUO model results in static urine flow and a rise in the hydrostatic pressure, which initially dilates the collecting ducts [19, 36]. Over the 10-day progression of UUO, hydrostatic pressure is transmitted back to the distal and proximal tubules [19]. The rise of pressure in proximal tubule decreases glomerular filtration rate and damages the tubular epithelial cells [37]. Renal tubular injury was evaluated in male and female ROP +/+ and low nephron number ROP *Os*/+ mice subjected to UUO. We found that UUO caused marked increase in the renal mRNA expression of the tubular injury marker NGAL in both ROP *Os*/+ and ROP +/+ mice. Male and female mice demonstrated a sex-independent effect of UUO on the renal tubular pathology in ROP mice. Our data also demonstrate that low nephron number did not affect UUO-induced tubular injury in these mice. Renal tubular injury was further assessed by studying the formation of renal tubular cast formation and found that kidney cast area was elevated in UUO-ROP +/+ compared to UUO-ROP *Os*/+ mice. Like our findings with NGAL expression, low nephron number and gender of the mice did not affect formation of UUO-induced renal tubular cast formation.

Renal tubular injury causes renal infiltration of leukocytes, mainly macrophages, T-lymphocytes, and neutrophils [24]. These infiltrating immune cells cause renal inflammation and

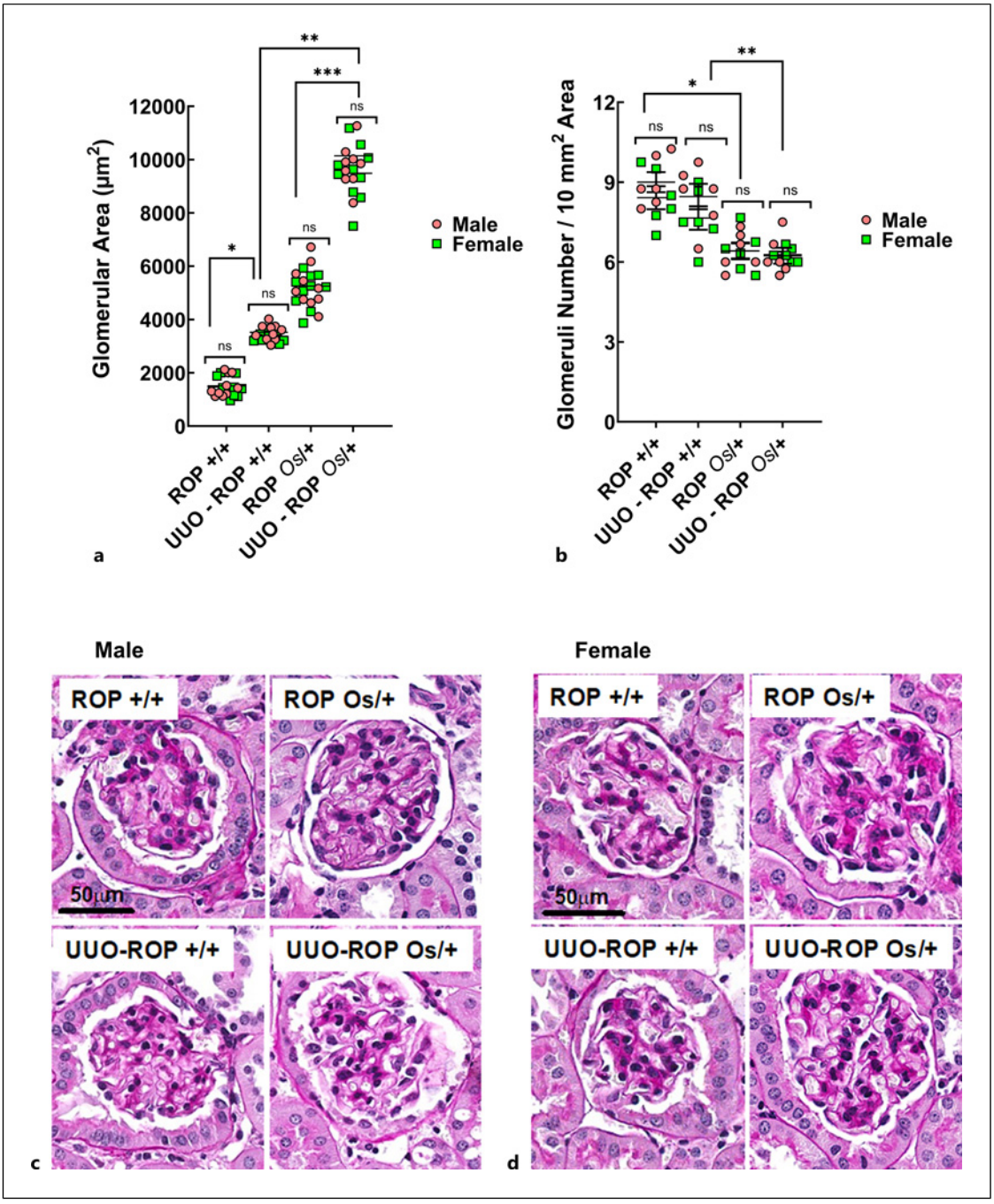

Fig. 7. Glomerular area and number of glomeruli in different experimental groups. Calculated glomerular area (**a**) and number (**b**) in the male and female ROP +/+ and ROP *Os*/+ mice with or without UUO. **c–d** Representative photomicrograph showing glomeruli in different experimental groups. Data were analyzed by 3-way ANOVA and presented in scattered plot format with mean and SEM. Data were analyzed by 3-way ANOVA and presented in scattered plot format with mean and SEM. The 3-way ANOVA was significant ($p < 0.05$) for genotype (ROP+/+ vs. ROP *Os*/+) but not ($p > 0.05$) for UUO and the sex of the mice. There was no was significant difference in glomerular tuft area between ROP +/+ versus UUO-ROP +/+ ($p > 0.05$ and indicated by "ns"), but there was significant difference between ROP *Os*/+ versus UUO-ROP *Os*/+ or between UUO-ROP +/+ versus UUO-ROP *Os*/+ (all $p < 0.05$). Number of glomeruli was lower in ROP *Os*/+ compared to ROP +/+ mice (#$p < 0.05$). **a** Glomerular area $n = 10$/group from a single experimental set. **b** Glomeruli number $n = 6$/group from a single experimental set; ns, not significant.

significantly contribute to the development and progression of renal fibrosis [19, 29]. Considering a critical role of inflammation in renal fibrosis pathogenesis, the current study examined renal inflammation in UUO-induced ROP +/+ and ROP *Os*/+ mice. Marked inflammation with infiltrated MAC2-positive macrophages in the kidney following UUO induction was evident in ROP +/+ and ROP *Os*/+ mice. As with renal fibrosis and tubular injury, renal inflammation was similar between male and female mice and greater in ROP +/+ compared to low nephron number ROP *Os*/+ mice.

A previous study comparing the renal transcriptomes of ROP +/+ and ROP *Os*/+ mice found increased oxidative stress and mitochondrial dysfunction linked to activation of transforming growth factor-β signaling in ROP *Os*/+ mice [38]. There have been a limited number of studies that have evaluated other diseases or factors that could enhance progressive kidney injury in the ROP *Os*/+ mice. One such study demonstrated that hyperlipidemia worsens renal pathology in ROP *Os*/+ mice through increased renal cytokines, platelet-derived growth factor, and transforming growth factor-β pathways [39]. Another study found that ROP *Os*/+ mice with a superimposed Fas-inactivating mutation (lymphoproliferative [lpr]) displayed more severe glomerular and tubulointerstitial disease [40]. Surprisingly, in our study, the UUO-induced renal fibrosis, tubular injury, and inflammation were not elevated in ROP *Os*/+ mice with reduced nephron number. However, in contrast to renal fibrosis and renal tubular injury, we found that glomerular tuft area was greater in ROP *Os*/+ compared to ROP +/+ mice following UUO. This finding is supported by an earlier study that reported glomerular hypertrophy in ROP *Os*/+ mice [18], and UUO is widely known to cause glomerular hypertrophy [10]. Unlike glomerular tuft area, glomeruli number was not affected by either sex or UUO. However, as reported earlier, the number of glomeruli was higher in the wild-type ROP +/+ than the mutant ROP *Os*/+ mice [15–18].

Conclusion

The current study investigated the development of UUO-induced renal fibrosis, tubular injury, and glomerular hypertrophy in male and female of two strains of mice. Our experimental findings demonstrate that development of renal fibrosis and tubular injury was not exacerbated by low nephron number or smaller kidney size. Interestingly, the findings demonstrate that ROP +/+ mice with normal kidney had higher renal fibrosis, tubular injury, and inflammation compared to low nephron number ROP *Os*/+ mice. Importantly, our data demonstrate that UUO-induced renal fibrosis, tubular injury, and inflammation were similar in male and female ROP +/+ and ROP *Os*/+ mice. In contrast to UUO-induced renal fibrosis and tubular injury, low nephron number enhanced UUO-induced glomerular hypertrophy in male and female ROP *Os*/+ mice compared ROP +/+. Overall, we demonstrate that low nephron number contributes to UUO-induced glomerular hypertrophy but not kidney fibrosis and tubular injury. We also demonstrate that none of the changes caused by UUO was affected by sex in any of the ROP mouse genotypes.

Acknowledgment

We acknowledge technical assistance of Tamas Krista of Department of Pharmacology and Toxicology at the Medical College of Wisconsin in analyzing RT-PCR data.

Statement of Ethics

The animal study was reviewed and approved by the Medical College of Wisconsin Institutional Animal Care and Use Committee, and the approval number was AUA 2323.

Conflict of Interest Statement

The authors have no conflicts of interest to declare.

Funding Sources

The National Institute of Diabetes and Digestive and Kidney Diseases grant DK103616, the National Center for Advancing Translational Sciences grant UL1 TR001436, and the Arkansas Research Alliance provided support to Ashraf El-Meanawy and John D. Imig.

Author Contributions

J.D.I., S.G., M.A.H.K., and A.E.-M. conceived the study, interpreted the data, and wrote the manuscript. S.G. and M.A.H.K. performed the experiments. All authors including A.M. edited the manuscript. All authors have read and agreed to the published version of the manuscript.

Data Availability Statement

The raw data supporting the conclusion of this article will be made available by the authors without undue reservation, and the public access of the data is not restricted, either legally or ethically. The correspondence author should be contacted for the raw data and for any further inquiry about the manuscript.

References

1 Kovesdy CP. Epidemiology of chronic kidney disease: an update 2022. Kidney Int. 2022;12(1):7–11.
2 Saran R, Robinson B, Abbott KC, Bragg-Gresham J, Chen X, Gipson D, et al. US renal data System 2019 annual data report: epidemiology of kidney disease in the United States. Am J Kidney Dis. 2020;75(1 Suppl 1):A6–A7.
3 Rhee CM, Kovesdy CP. Epidemiology: spotlight on CKD deaths—increasing mortality worldwide. Nat Rev Nephrol. 2015;11(4):199–200.
4 GBD Chronic Kidney Disease Collaboration. Global, regional, and national burden of chronic kidney disease, 1990-2017: a systematic analysis for the Global Burden of Disease Study 2017. Lancet. 2020;395(10225):709–33.
5 Neugarten J. Gender and the progression of chronic kidney disease. Mayo Clin Proc. 2020;95(12):2582–4.
6 Ricardo AC, Yang W, Sha D, Appel LJ, Chen J, Krousel-Wood M, et al. Sex-related disparities in CKD progression. J Am Soc Nephrol. 2019;30(1):137–46.
7 Cain JE, Di Giovanni V, Smeeton J, Rosenblum ND. Genetics of renal hypoplasia: insights into the mechanisms controlling nephron endowment. Pediatr Res. 2010;68(2):91–8.
8 Chevalier RL, Forbes MS, Thornhill BA. Ureteral obstruction as a model of renal interstitial fibrosis and obstructive nephropathy. Kidney Int. 2009;75(11):1145–52.
9 Martínez-Klimova E, Aparicio-Trejo OE, Tapia E, Pedraza-Chaverri J. Unilateral ureteral obstruction as a model to investigate fibrosis-attenuating treatments. Biomolecules. 2019;9(4):141.
10 Klahr S, Morrissey J. Obstructive nephropathy and renal fibrosis. Am J Physiol Ren Physiol. 2002;283(5):861–75.
11 Ruiz-Ortega M, Rayego-Mateos S, Lamas S, Ortiz A, Rodrigues-Diez RR. Targeting the progression of chronic kidney disease. Nat Rev Nephrol. 2020;16(5):269–88.
12 Kalantar-Zadeh K, Li PK. Strategies to prevent kidney disease and its progression. Nat Rev Nephrol. 2020;16(3):129–30.
13 Fattah H, Layton A, Vallon V. How do kidneys adapt to a deficit or loss in nephron number? Physiology. 2019;34(3):189–97.
14 Schnaper HW. Remnant nephron physiology and the progression of chronic kidney disease. Pediatr Nephrol. 2014;29(2):193–202.
15 Esposito C, He CJ, Striker GE, Zalups RK, Striker LJ. Nature and severity of the glomerular response to nephron reduction is strain-dependent in mice. Am J Pathol. 1999;154(3):891–7.
16 Wang Y, Heilig KO, Minto AW, Chen S, Xiang M, Dean DA, et al. Nephron-deficient Fvb mice develop rapidly progressive renal failure and heavy albuminuria involving excess glomerular GLUT1 and VEGF. Lab Invest. 2010;90(1):83–97.
17 Zalups RK. The *Os*/+ mouse: a genetic animal model of reduced renal mass. Am J Physiol. 1993;264(1 Pt 2):F53–60.
18 Cho MH, Jung KJ, Jang HS, Kim JI, Park KM. Orchiectomy attenuates kidney fibrosis after ureteral obstruction by reduction of oxidative stress in mice. Am J Nephrol. 2012;35(1):7–16.
19 Metcalfe PD, Leslie JA, Campbell MT, Meldrum DR, Hile KL, Meldrum KK. Testosterone exacerbates obstructive renal injury by stimulating TNF-alpha production and increasing proapoptotic and profibrotic signaling. Am J Physiol Endocrinol Metab. 2008;294(2):E435–43.
20 Tingskov SJ, Jensen MS, Pedersen CET, de Araujo IBBA, Mutsaers HAM, Nørregaard R. Tamoxifen attenuates renal fibrosis in human kidney slices and rats subjected to unilateral ureteral obstruction. Biomed Pharmacother. 2021;133:111003.
21 Tofteng SS, Nilsson L, Mogensen AK, Nørregaard R, Nüsing R, Diatchikhine M, et al. Increased COX-2 after ureter obstruction attenuates fibrosis and is associated with EP2 receptor upregulation in mouse and human kidney. Acta Physiol. 2022;235(4):e13828.
22 Sharma A, Hye Khan MA, Levick SP, Lee KS, Hammock BD, Imig JD. Novel omega-3 fatty Acid epoxygenase metabolite reduces kidney fibrosis. Int J Mol Sci. 2016;17(5):751.
23 Skibba M, Hye Khan MA, Kolb LL, Yeboah MM, Falck JR, Amaradhi R, et al. Epoxyeicosatrienoic Acid analog decreases renal fibrosis by reducing epithelial-to-mesenchymal transition. Front Pharmacol. 2017;8:406.
24 Cao Q, Harris DC, Wang Y. Macrophages in kidney injury, inflammation, and fibrosis. Physiology. 2015;30(3):183–94.
25 Wise TL, Pravtcheva DD. Oligosyndactylism mice have an inversion of chromosome 8. Genetics. 2004;168(4):2099–112.
26 Liu Y. Renal fibrosis: new insights into the pathogenesis and therapeutics. Kidney Int. 2006;69(2):213–7.
27 Moeller MJ, Kramann R, Lammers T, Hoppe B, Latz E, Ludwig-Portugall I, et al. New aspects of kidney fibrosis-from mechanisms of injury to modulation of disease. Front Med. 2021;8:814497.
28 Humphreys BD. Mechanisms of renal fibrosis. Annu Rev Physiol. 2018;80:309–26.
29 Bülow RD, Boor P. Extracellular matrix in kidney fibrosis. More than just a scaffold. J Histochem Cytochem. 2019;67(9):643–61.
30 Kim J, Imig JD, Yang J, Hammock BD, Padanilam BJ. Inhibition of soluble epoxide hydrolase prevents renal interstitial fibrosis and inflammation. Am J Physiol Renal Physiol. 2014;307(8):F971–80.
31 Teng S, Liu G, Li L, Ou J, Yu Y. CUX1 promotes Epithelial-Mesenchymal Transition (EMT) in renal fibrosis of UUO model by targeting MMP7. Biochem Biophys Res Commun. 2022;608:128–34.
32 Yuan Q, Tan RJ, Liu Y. Myofibroblast in kidney fibrosis: origin, activation, and regulation. Adv Exp Med Biol. 2019;1165:253–83.
33 Nakagawa N, Duffield JS. Myofibroblasts in fibrotic kidneys. Curr Pathobiol Rep. 2013;1(3):189–98.
34 Swartling O, Rydell H, Stendahl M, Segelmark M, Trolle Lagerros Y, Evans M. CKD progression and mortality among men and women: a nationwide study in Sweden. Am J Kidney Dis. 2021;78(2):190–9.e1.
35 Falke LL, Broekhuizen R, Huitema A, Maarseveen E, Nguyen TQ, Goldschmeding R. Tamoxifen for induction of Cre-recombination may confound fibrosis studies in female mice. J Cell Commun Signal. 2017;11(2):205–11.
36 Black LM, Lever JM, Agarwal A. Renal inflammation and fibrosis: a double-edged sword. J Histochem Cytochem. 2019;67(9):663–81.
37 Mühlfeld AS, Spencer MW, Hudkins KL, Kirk E, LeBoeuf RC, Alpers CE. Hyperlipidemia aggravates renal disease in B6.ROP Os/+ mice. Kidney Int. 2004;66(4):1393–402.
38 El-Meanawy A, Schelling JR, Iyengar SK, Hayden P, Barathan S, Goddard K, et al. Identification of nephropathy candidate genes by comparing sclerosis-prone and sclerosis-resistant mouse strain kidney transcriptomes. BMC Nephrol. 2012;13:61.
39 Jarad G, Lakhe-Reddy S, Blatnik J, Koepke M, Khan S, El-Meanawy MA, et al. Renal phenotype is exacerbated in *Os* and *lpr* double mutant mice. Kidney Int. 2004;66(3):1029–35.
40 He C, Esposito C, Phillips C, Zalups RK, Henderson DA, Striker GE, et al. Dissociation of glomerular hypertrophy, cell proliferation, and glomerulosclerosis in mouse strains heterozygous for a mutation (*Os*) which induces a 50% reduction in nephron number. J Clin Invest. 1996;97(5):1242–9.